



Effect of Reedy Emergent Side-Vegetation in Gravel-Bed Streams on Bed Shear Stress: Patch Scale Analysis

Parisa Setayesh¹ · Hossein Afzalimehr²

Received: 27 June 2020 / Accepted: 7 April 2021 / Published online: 22 April 2021
© Shiraz University 2021

Abstract

Vegetation in open channels alters turbulent and other hydraulic characteristics of flow. Hence, conventional methods for computing bed shear stress in bare channels are not applicable in such channels. The present study, therefore, experimentally investigates the distributions of velocity in 3D in gravel bed channels with vegetation and investigates six different methods for estimating bed shear stress. The distribution of shear stress is basically controlled by the spatial distribution of vegetation as well as the biomechanical and architectural features of these plants. It is found that near the bottom of the flume, the shear stress changes in dense layers, constituting a layered shape.

Keywords Bed shear stress · Drag coefficient · Gravel bed channels · Vegetation · Open channel flow · Emergent vegetation

List of Symbols

A_v	Frontal projected area of the stem for the emergent vegetation
Br	Numerical constant of integration
C_D	Drag coefficient
D	Frontal projected
d_{50}	Median diameter of sediment particles
H	Flow depth
g	Gravitational acceleration
K	Karman's universal constant ($k=0.4$)
k_s	Equivalent sand roughness
m	Vegetation density
s	Energy slope that is equal to bed slope in uniform flow
U'	RMS value of the velocity fluctuation in the longitudinal direction
U	The velocity components in the streamwise direction (mean velocity)
U_*	Shear velocity

U_f	Turbulence fluctuations in the longitudinal directions
V'	RMS value of the velocity fluctuation in the transverse direction
V	The velocity components in the transverse direction
W'	RMS value of the velocity fluctuation in the vertical direction
W	The velocity components in the vertical direction
W_f	Turbulence fluctuations in the vertical directions
z	Axis perpendicular to the bed
Z	Flow depth from the bed of channel
z/H	Relative flow depth
ρ	Water density
τ_0	Bed shear stress
τ_{Rey}	Local Reynolds stress
τ_t	Total shear stress
τ_{vis}	Local viscous stress
ϑ	Kinematic viscosity of flow

✉ Parisa Setayesh
psetayesh.iut@gmail.com
Hossein Afzalimehr
hafzali@iust.ac.ir

¹ Department of Water Engineering, Isfahan University of Technology, Isfahan, Iran

² Department of Civil Engineering, Iran University of Science and Technology, Tehran, Iran

1 Introduction

Estimation of hydraulic resistance of natural rivers with an acceptable accuracy is the key issue in design of hydraulic problems. The bed shear stress in bare channels without vegetation can be estimated with several methods, but most of these are not appropriate for vegetated channels due to the impact of vegetation on the velocity profile and turbulence production (Yang et al. 2015). Bed shear stress can

be estimated by using the vertical velocity distribution for non-vegetated flow. However, in flow domains, where the flow passes over/around/trough vegetation, turbulent flow characteristics are largely dictated by the plants. Hence, the standard methods which are employed to calculate the bed shear stress on as bare bank or bare bed conditions are not applicable (Huai et al. 2014; Klopstra et al. 1997; Righetti 2008 and Wilson 2007).

The hydraulic resistance of flow with vegetation depends not only on bed roughness, but also on vegetation-induced drag (Tang et al. 2014). In such natural rivers, over vegetation, the viscous stress is negligible and total stress largely composed of Reynolds stress which is originated from vegetation. Hamidfar et al. 2020 experimentally investigated the influence of rigid emerged vegetation in a channel bend on the bed shear stress, mean flow, bend scour and flow velocity. They reported that the emergent vegetation extremely affect the flow direction, turbulent kinetic energy and bed shear stress and the corresponding bed topography in the channel bend (Hamidfar et al. 2020). In fact, there is a general consistency in the pertinent literature that vegetation alters not only the turbulence, secondary flow pattern and velocity distribution, but also the structure of the boundary layer in rivers as well. This situation renders the known laws, including the log law, invalid. The authors have investigated the effect of vegetation on the velocity and shear stress in different works (Afzalimehr and Dey 2009, 2010a,b, Nasiri et al. 2010, Nasiri et al. 2011, Afzalimehr et al. 2012, Fazlollahi et al. 2015a, Fazlollahi et al. 2015b, Afzalimehr et al. 2016, Afzalimehr and Setayesh 2018 and Shahmohammadi et al. 2018). They found a significant influence of vegetation on the hydraulic parameters, and the results obtained in laboratory scale such as the logarithmic law and the Reynolds stress distribution can be extended to the prototype, i.e., river scale regardless of width-to-depth ratio. However, the presence of reedy vegetation across the flow has been less considered on the flow velocity and Reynolds stress distributions. The assumptions consist of steady and quasi-uniformity of flow, no obstacle and submerged vegetation and bed form along the stream.

Follet and Nepf (2012) investigated the sediment patterns formed in a sand bed around circular patches of reedy emergent vegetation using the bed shear stress formula ($\tau_0 = \rho U_*^2$) to describe the threshold of sediment motion. This is followed the study by Yagci et al. (2016 and 2017), who demonstrated the role of the plant architecture/morphometry on scour morphology which emerge as a consequence of the increased near bottom turbulence and bed shear stress. They observed that with the decreasing permeability of plant, the scour hole localized and due to the effect of bending (i.e., streamlining) of the plant scour decreases considerably despite its increased submerged volume. Sellin and van Beesten (2004) also demonstrated that the hydraulic

resistance of a typical natural river is highly variable depending on the season. Yang et al. (2015) suggested a new model to obtain bed shear stress in both vegetated and bare channels with smooth beds and rigid dowels as emergent vegetation. The flow structure observed in vegetated channels is greatly three-dimensional (Tang et al. 2014). Therefore, the velocity components in the vertical direction, W , and in the transverse direction, V , are significant.

In submerged vegetation case, the flow is generally divided into two layers (Klopstra et al. 1997; Neary 2003; Shimizu and Tsujimoto 1994; Wilson et al. 2006a and 2006b; Tang 2014), the lower layer is specified by the flow through the vegetation and the upper one by the flow above the top of vegetation (Huai et al. 2009 and Righetti and Armanini, 2002). However, the flow through the emergent vegetation shows different pattern because plants cover the whole depth (Kitsikoudis et al., 2016 and 2020). This makes difficult to apply some traditional methods to estimate the bed shear stress in such cases. This study investigates the flow velocity gradient for vegetation and the non-vegetation zones in x -, y - and z -directions in a laboratory flume.

The step-by-step procedure is described in the next part of the "Introduction" and "Materials and Methods" sections.

Shear velocity is obtained from the momentum equation to consider how emergent vegetation influences the flow structures.

The momentum equation for two-dimensional, steady and uniform flow in a gravel channel bed can be expressed as:

$$\frac{\partial \tau_t}{\partial z} + \rho g s = 0 \quad (1)$$

where τ_t is the total shear stress, z is axis perpendicular to the bed, ρ is the water density, g is the gravitational acceleration and s is the energy slope that is equal to bed slope in uniform flow.

Total shear stress is expressed as, $\tau_t = \tau_{\text{Rey}} + \tau_{\text{vis}}$ where $\tau_{\text{Rey}} = -\rho \overline{U_f W_f}$ is the local Reynolds stress and $\tau_{\text{vis}} = \rho \nu \frac{dU}{dz}$ is the local viscous stress, where (U_f) is the turbulence fluctuations in the longitudinal, (W_f) is the turbulent fluctuation in the vertical directions and ν is the kinematic viscosity. The viscous stress exists in a very thin sublayer close to the bed where ADV cannot be used to collect data, but U varies over the flow depth and $\frac{dU}{dz}$ exists significantly because of turbulent boundary layer (see Fig. 3). This study proposes the calculation of $\frac{dU}{dz}$ as $\frac{dU}{dz} = \frac{U_i - U_{i-1}}{z_i - z_{i-1}}$ and investigates the influence of $\frac{dU}{dz}$ on the Reynolds stress.

The change in the total stress in the vertical direction can be expressed as:

$$\frac{\partial \tau_t}{\partial z} = \frac{\partial}{\partial z} \left(\rho \nu \frac{dU}{dz} - \rho \overline{U_f W_f} \right) \quad (2)$$

Methods for estimation of bed shear stress:

Method 1 There are different methods to estimate bed shear stress in the literature (Dey 2014). The first method is the slope method: ($\tau_0 = \rho g s H$), where τ_0 is the bed shear stress, ρ is the water density, g is the gravitational acceleration, s is the energy slope and H is the flow depth. This method is applied in bare channels (Yang et al. 2015) with high width.

Method 2 The second method was the log-law method: $\tau_0 = \rho U_*^2$, where U_* is obtained from the log-law (Eq. 3):

$$\frac{U}{U_*} = \frac{1}{k} \ln \left(\frac{z}{k_s} \right) + Br \quad (3)$$

where U is the mean velocity, U_* is the shear velocity, k is Karman's universal constant ($k = 0.4$), z is flow depth from the bed of channel, k_s is the equivalent sand roughness that is assumed in this study $k_s = d_{50}$ and Br is a numerical constant of integration (Graf and Altinakar 1998).

Method 3 The third method is the Reynolds stress method: ($\tau_0 = -\rho \overline{U_f W_f}$) near the bottom of flume which uses the turbulence fluctuations in the longitudinal (U_f) and vertical (W_f) directions.

Method 4 The fourth method is the drag method: ($\tau_0 = -\rho C_D U^2$) (Biron et al. 2004), where drag coefficient is $C_D = \frac{2U_f W_f}{U^2}$, leading to ($\tau_0 = 2\rho \overline{U_f W_f}$).

Method 5 The fifth method is the TKE method with $C_1 = 0.19$ (Dey 2014) expresses as:

$$\tau_0 = C_1 \left[0.5\rho \left(\overline{U'^2} + \overline{V'^2} + \overline{W'^2} \right) \right] \quad (4)$$

where U' is the RMS value of the velocity fluctuation in the longitudinal direction, V' is the RMS value of the velocity fluctuation in the transverse direction and W' is the RMS value of the velocity fluctuation in the vertical direction.

Method 6 The sixth method is the TKEW' method with $C_2 = 0.9$ (Biron et al. 2004) expresses as:

$$\tau_0 = C_2 \left[\rho \left(\overline{W'^2} \right) \right] \quad (5)$$

The present study therefore experimentally investigates the distributions of velocity components in 3D.

This study employs six different methods to estimate the bed shear stress in gravel-bed channels and reedy emergent vegetation channels in order to present a convenient method to estimate bed shear stress. The effect of reedy vegetation and its density on the velocity and Reynolds stress distributions in a gravel-bed river in the main novelty of the present work.

The objective of this research is to investigate the role of reedy vegetation on the shear stress estimation via studying the flow characteristics in a gravel-veg stream. The sort of reedy vegetation, the size of grain size (gravel) and its distribution with a geometric standard deviation less than

1.4, the approximate flow depth, the density of vegetation is among the characteristics of Kaj River which were used in this laboratory work.

There were considerable emergent vegetation covers in different locations through in the selected reach of the Kaj River. This helped to simulate part of this reach in the laboratory, considering limitation of width, aspect ratio, assuming the quasi-uniform flow condition and no obstacle (boulder) in the selected reach.

The measuring sections were selected based on the fully developed condition in the flume, which was determined by adapting the dimensionless velocity profiles in this interval by experimental data from presented research and previous research in this flume (Afzalimehr et al. 2019a, b, Barahimi and Afzalimehr 2019, Fazlollahi et al. 2015a, Fazlollahi et al. 2015b, Nasiri et al. 2013 and Nasiri et al. 2011).

The distance between the rows of emergent vegetation is 20 cm, and the distance between the columns of emergent vegetation is 2 cm. The ADV device is placed between the rows of emergent vegetation, so there is no problem for data collection.

There are few studies in this area in the literature, demanding more investigation to analyze the role of arrangement of reedy emergent vegetation on the flow characteristics in gravel-bed streams.

2 Materials and Methods

The experiments were conducted in a rectangular flume 8 m long, 0.4 m wide and 0.6 m deep in the Water Research Center Laboratory at the Isfahan University of Technology, Iran. Many researchers conducted their experiments in this flume previously (Afzalimehr et al. 2019a, b, Barahimi and Afzalimehr 2019, Fazlollahi et al. 2015a, Fazlollahi et al. 2015b, Afzalimehr and Setayesh 2018, Nasiri et al. 2013 and Nasiri et al. 2011). The effect of the width of the flume is observed in the velocity and Reynolds stress distributions. The dip phenomenon shows the effect of walls of flume in which the maximum velocity occurs under the water surface (Afzalimehr and Dey 2009). Almost all laboratory studies have aspect ratio (width-to-depth ratio) less than 5 in; however, they are used for gravel-bed rivers modeling with large aspect ratio. This limitation in laboratory studies is not significant because the main laws of hydraulics including the log-law are independent of aspect ratio. Many authors already were conducted the experiment in this flume with width of 40 cm and published articles in valuable journals (Afzalimehr et al. 2019a, b, Barahimi and Afzalimehr 2019, Fazlollahi et al. 2015a, Fazlollahi et al. 2015b, Nasiri et al. 2013 and Nasiri et al. 2011). For example, Afzalimehr et al. (2016) used a flume with width of 30 cm to show the general pattern of Reynolds stress and the flow velocity.

The authors arranged a field visit and observed in several gravel-bed rivers including Kaj River in Iran and found many small vegetation patches distributed randomly. This was one of the main reasons to carry out the present research in a gravel-bed river. The range of flow parameters, bed material (i.e., d_{50}) and the vegetation condition (i.e., emergent and reedy vegetation) were selected based on the real conditions of Kaj River in Shahrekord, central Iran. The selected grain size and reedy vegetation in this study are frequently observed in Kaj River and influence the hydraulic parameters estimation. The assumption is the flow is steady and quasi-uniform, the vegetation is not flexible, and the standard deviation of gravel size is less 1.4 showing the bed material are uniformly distributed. The flume had glass walls and glass bottom covered by gravel having a median size $d_{50} = 1.72$ cm which was calculated based on Wolman's method (1954) in the Kaj River, and other parts with reedy emergent vegetation with a diameter $D = 0.01$ m and height $H_v = 0.35$ m. The selected particle size shows the median grain size in our previous field studies in some reaches of Kaj River. The results are valid for gravel-bed streams. This means no matter 1.7 cm or 2.7 cm because no change is observed in boundary layer characteristics as long as one works in gravel range. No cobble and boulder was observed in the selected reach. This is done in many river engineering projects. For example, the authors found the particle size 22 mm for Zayandehroud River in Isfahan. This depends on the selected reach in any river and its geometric standard deviation. A tail gate located at the end of the flume controlled the water level at 0.2 m depth during the experiments. To ensure the generation of fully developed turbulent flow, experiments were carried out long enough, far from the inlet $L = 5.5$ to $L = 6.5$ m. This was controlled by repeating the

results of velocity distributions in different distances from the flume entrance. The authors used this method in many studies for more than 25 years and presenting the results in international journals. There is no back water in the flume and the gate at the end of channel does not affect the results (Afzalimehr et al. 2019a, b, Barahimi and Afzalimehr 2019, Fazlollahi et al. 2015a, Fazlollahi et al. 2015b, Nasiri et al. 2013 and Nasiri et al. 2011). Velocity profiles have also been investigated in this region to ensure fully flow development. The preliminary tests clearly verified that the flow was fully developed before the flow attain to vegetated section. A wave dissipation board was located upstream of the flume to decrease the inlet turbulence to have the uniform flow.

A pump with a maximum discharge of $0.050 \text{ m}^3/\text{s}$ (q_{\max}), circulated water from a constant elevation sump and an electromagnetic flow-meter was installed on the supply conduit connected to the flume to continuously measure the discharge passing through the channel. The flow discharge was kept constant as $0.035 \text{ m}^3/\text{s}$ throughout this study. Water depths were measured with a mobile limnimeter along the flume to verify the flow quasi-uniformity. To simulate emergent vegetation, rigid and woody circular cylinders were arranged in an array next to the right wall of flume (Fig. 1). $L_v = 0.2$ m is the spacing between the rigid vegetation in the streamwise direction and B_v in the lateral direction which is varying from 0.02 to 0.11 m in the all densities. Four rows of vegetation were considered in the flume (see Fig. 2). This is enough for a study in laboratory because in general the measuring process is concentrated on the specific section of the flume. This is confirmed by the previous works by the authors and other researchers. For example, the referee may kindly address to Shahmammadi et al. (2018) and Jahadi

Fig. 1 View of gravel bed and emergent vegetation. Nine experiments were conducted only over non-vegetation gravel bed and other experiments were carried out on vegetation gravel bed with five different densities



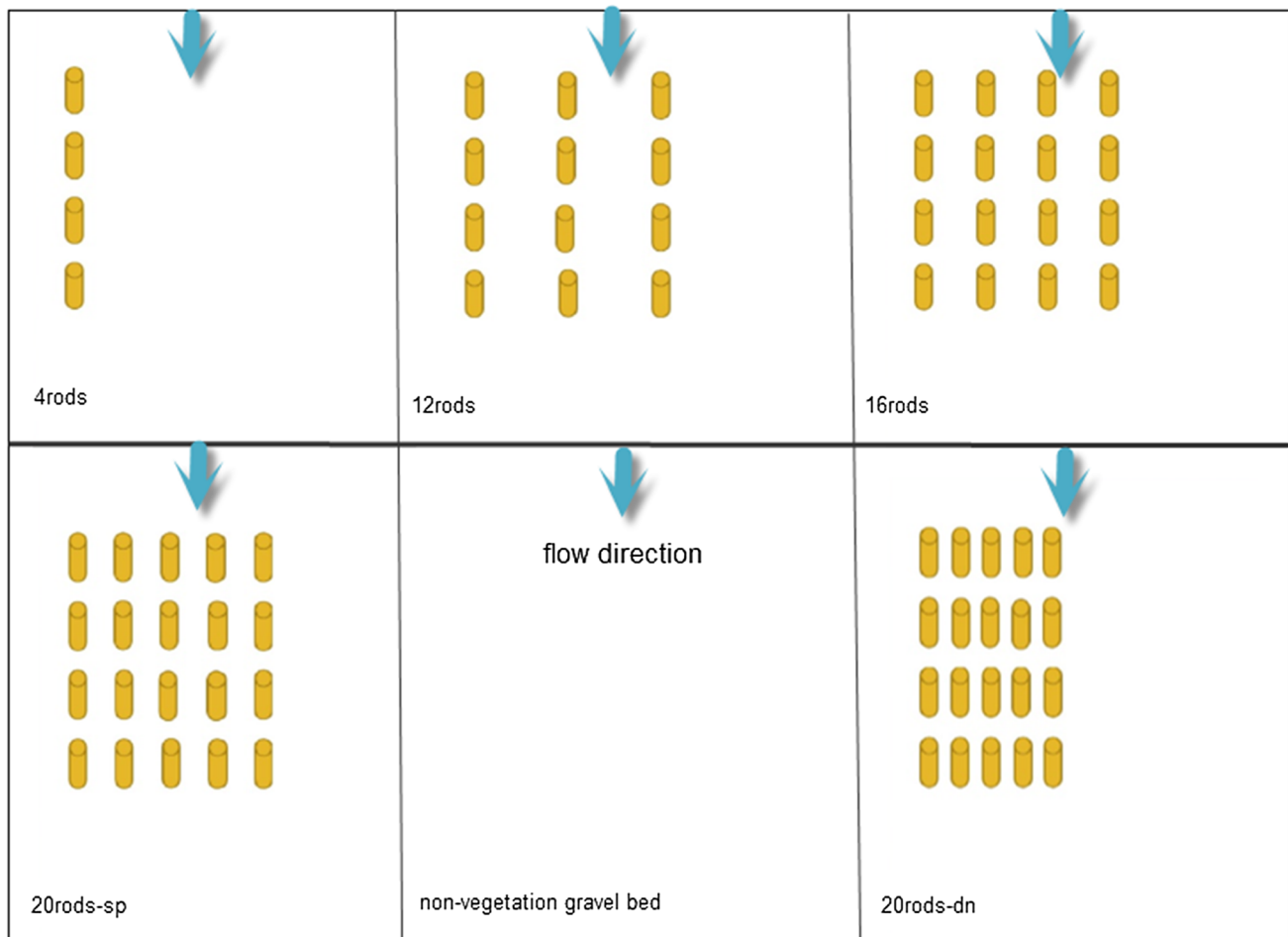


Fig. 2 The distribution of rods in different configurations of vegetated zone

et al. (2020). Based on the channel width, these densities were considered in this study.

For a circular patch with cylindrical wooden rods to decrease the influence of walls on the flow near the patch, Follett and Nepf (2012) suggested the maximum patch diameter is 0.18 of the channel width ($\frac{D_p}{B} = 0.18$). In the present study, a rectangular patch was used with woody cylinders and ($0.15 < \frac{D_p}{B} < 0.67$). Since the geometric shapes of vegetation are various in the nature, the vertical cylinders were considered to present the geometry of vegetation in this study as reported by Tang et al. 2014 and Thompson et al. 2004 in laboratory studies.

To measure velocity components (U , V , W) and turbulence characteristics (U' , V' , W'), a three-dimensional acoustic Doppler velocimetry (ADV) was used at sampling frequency of 200 Hz. Based on the analysis given by Yagci et al. 2008 on influence of sampling number on turbulence statistics, to collect unbiased velocity data, the sampling duration was kept as 120 s at each measurement point of the velocity profile. In this way, 24,000 samples

were collected for each point measuring velocity during 120 s and was analyzed and filtered by WINADV software by using Goring and Nikora's method (2002). Distribution of sampling points was located in the middle of each patch.

The distance between each vegetation row was 0.2 m which was standard to use ADV device. In each density, ADV was placed in middle of rows. ADV could not measure data near the water surface. Also, collecting data is not easy very near the reedy vegetation. It is very difficult to keep the scale of model and prototype, especially, the aspect ratio.

The mesh dimension was standard and compared with the existing studies in the literature (Afzalimehr et al. 2019a, b, Barahimi and Afzalimehr 2019 and Afzalimehr and Setayesh 2018). The distance reedy vegetation row was 0.2 m and their lateral distance was 0.02 m. ADV was located between the rows, showing SNR larger than 15 and correlation coefficient larger than 95 percent for measuring 3D velocities without observing any significant noise in data time series.

3 Results

3.1 Shear Velocity

Equation (2) gives the vertical variation of total stress. For the non-vegetated gravel bed (Fig. 3a), the vertical variation of local Reynolds stress (τ_R), local viscous stress (τ_v) and total shear stress (τ_t) were given. It is seen from Fig. 3 that the viscous stress changes just in the inner layer ($\frac{z}{H} < 0.2$) near the wall, but it is constant in the outer layer ($\frac{z}{H} > 0.2$). Its maximum value occurs at the bed in all of cases. Figure 3b–f shows that in vegetation cases, the viscous stress changes over ($\frac{z}{H} < 0.05$) and remains constant above this relative depth. Therefore, the influence of viscous stress is negligible on the total stress and the Reynolds stress is applied to data analysis. Since there are a few data collections in $z/H < 0.05$ region, therefore, the influence of viscous stress may not be considered in this study.

Because there were four rows for reedy vegetation through the flume and ADV was located between the rows. There are four rows in each density. So there are three spaces between the rows in which the data are collected. Also, the result presented is the average of the results of each row in Fig. 3.

Equation 6 was obtained from Eq. 1 and Eq. 2 for gravel bed. The gravel bed has one layer over water depth and far from the vertical walls, Therefore, the integration of Eq. 6 from $z=0$ (bed) to $z=H$ (the flow surface) gives:

$$\frac{\partial}{\partial z} \left(\rho v \frac{dU}{dz} - \rho \overline{U_f W_f} \right) + \rho g s = 0 \quad (6)$$

$$\int_0^H \left(\frac{\partial}{\partial z} \left(\rho v \frac{dU}{dz} - \rho \overline{U_f W_f} \right) \right) dz + \int_0^H \rho g s dz = 0 \quad (7)$$

$$v \frac{dU}{dz} - \overline{U_f W_f} + = - g s H \quad (8)$$

where $U_* = \sqrt{g s H}$ is the shear velocity and obtains from Eq. 9 as:

$$U_* = \sqrt{\frac{1}{\rho} (\tau_{\text{Rey}} - \tau_{\text{vis}})} \quad (9)$$

For vegetation flow we can rewrite Eq. 1 as Eq. 10 (Huai et al. 2014):

$$\frac{\partial \tau}{\partial z} + \rho g s - F_D = 0 \quad (10)$$

where $F_D = \frac{1}{2} \rho C_D m D U^2$ is the vegetation drag force (Huai et al. 2014), $m = \frac{1}{L_v B_v}$ is the vegetation density, the distance between the vegetation in the streamwise direction is $L_v = 0.2$ and in the lateral direction is B_v , D is the frontal projected width of the stem, U is the mean streamwise

velocity and $C_D = \frac{2 \overline{U_f W_f}}{U^2}$ is the drag coefficient. So the total shear stress can be written as:

$$\frac{\partial}{\partial z} \left(\rho v \frac{dU}{dz} - \rho \overline{U_f W_f} \right) + \rho g s - \rho \overline{U_f W_f} m D = 0 \quad (11)$$

The total shear stress in vegetation cases have two layers, so we integrate Eq. 11:

$$\int_0^{0.2H} \left(\frac{\partial}{\partial z} \left(\rho v \frac{dU}{dz} - \rho \overline{U_f W_f} \right) + \rho g s - \rho \overline{U_f W_f} m D \right) dz + \int_{0.2H}^H \left(\frac{\partial}{\partial z} \left(\rho v \frac{dU}{dz} - \rho \overline{U_f W_f} \right) + \rho g s - \rho \overline{U_f W_f} m D \right) dz = 0 \quad (12)$$

$$U_* = \begin{cases} \sqrt{\frac{1}{0.2\rho} [(1 + 0.2mA_v)\tau_{\text{Rey}} - \tau_{\text{vis}}]} & \frac{z}{H} < 0.2 \\ \sqrt{\frac{1}{0.8\rho} [(1 + 0.8mA_v)\tau_{\text{Rey}} - \tau_{\text{vis}}]} & \frac{z}{H} > 0.2 \end{cases} \quad (13)$$

where $A_v = HD$ for the emergent vegetation is the frontal projected area of the stem. The shear velocity U_* , is obtained from Eq. 9 and Eq. 13 and contours of shear velocity in the cross section of flume are drawn in Fig. 4. The maximum value of shear stress is on the bed of flume and decreases toward water surface which is plausible. From Fig. 4, near the bottom of flume, the shear stress changes greatly so layers are denser and appear like an onion shape that we called "Shear onion." Onion shape means being layered similar to onion layers. Shear onion on the gravel bed rises a little from the bottom of flume in the ax axes and it is not complete. Ax axes are the axis which is located in the middle of the flume width. With the addition of vegetation to gravel bed, in the first densities (4 rods), the shear onion appeared in the ax axes completely. For cases of 12 rods and 16 rods the shear onion grew and spread all over the flume bottom. For cases of 20 rods-sp and 20 rods-dn, the shear onion was divided into shear onions more on the bottom and walls of flume. In the vegetation cases, the shear onion happened in $\frac{z}{H} < 0.3$ and after that changes reduced. The vegetation was placed near the right wall of flume but shear onion appeared independent of region of vegetation.

3.2 Bed Shear Stress

Six methods were investigated to obtain bed shear stress for non-vegetation gravel bed and vegetation gravel bed (see Fig. 5 and Table. 1).

From the slope method: ($\tau_0 = \rho g s H$), the highest bed shear stress values and the highest shear velocity values were obtained in the abscissa for gravel bed and 4 rods density (Fig. 4 and 5). For the other vegetation cases, the bed shear

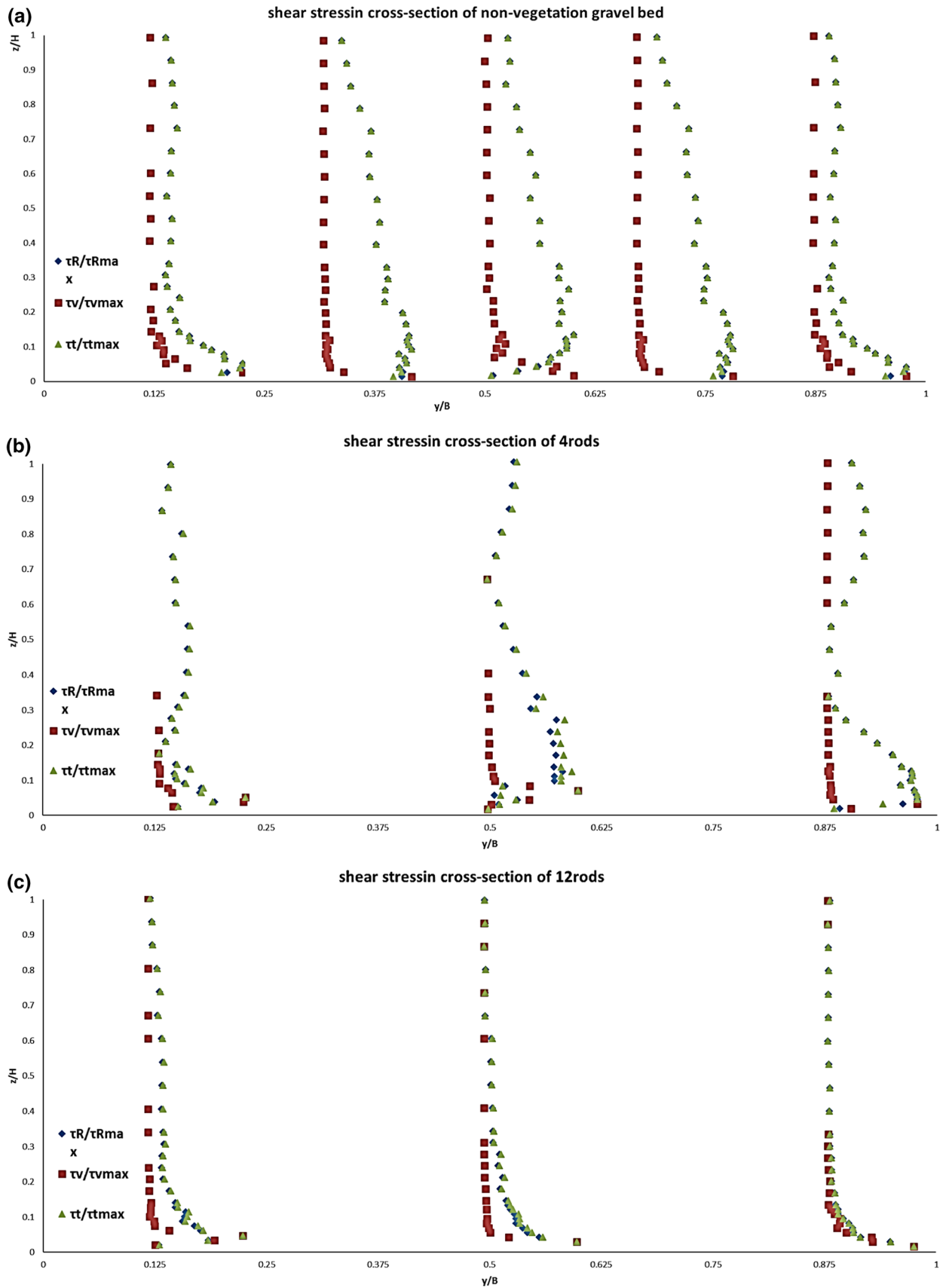


Fig. 3 Local Reynolds stress (τ_R), local viscous stress (τ_v) and total shear stress (τ_t)

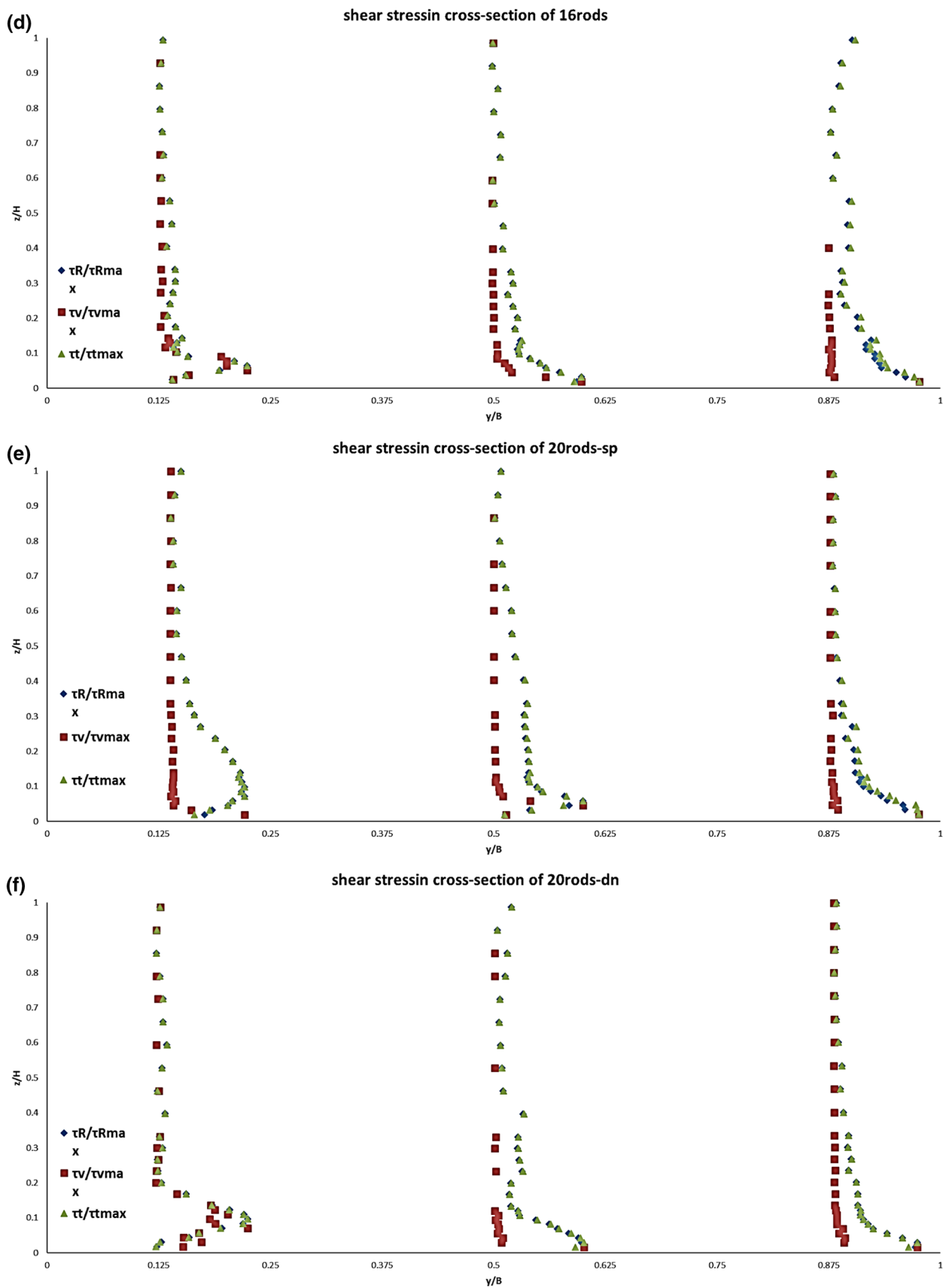


Fig. 3 (continued)

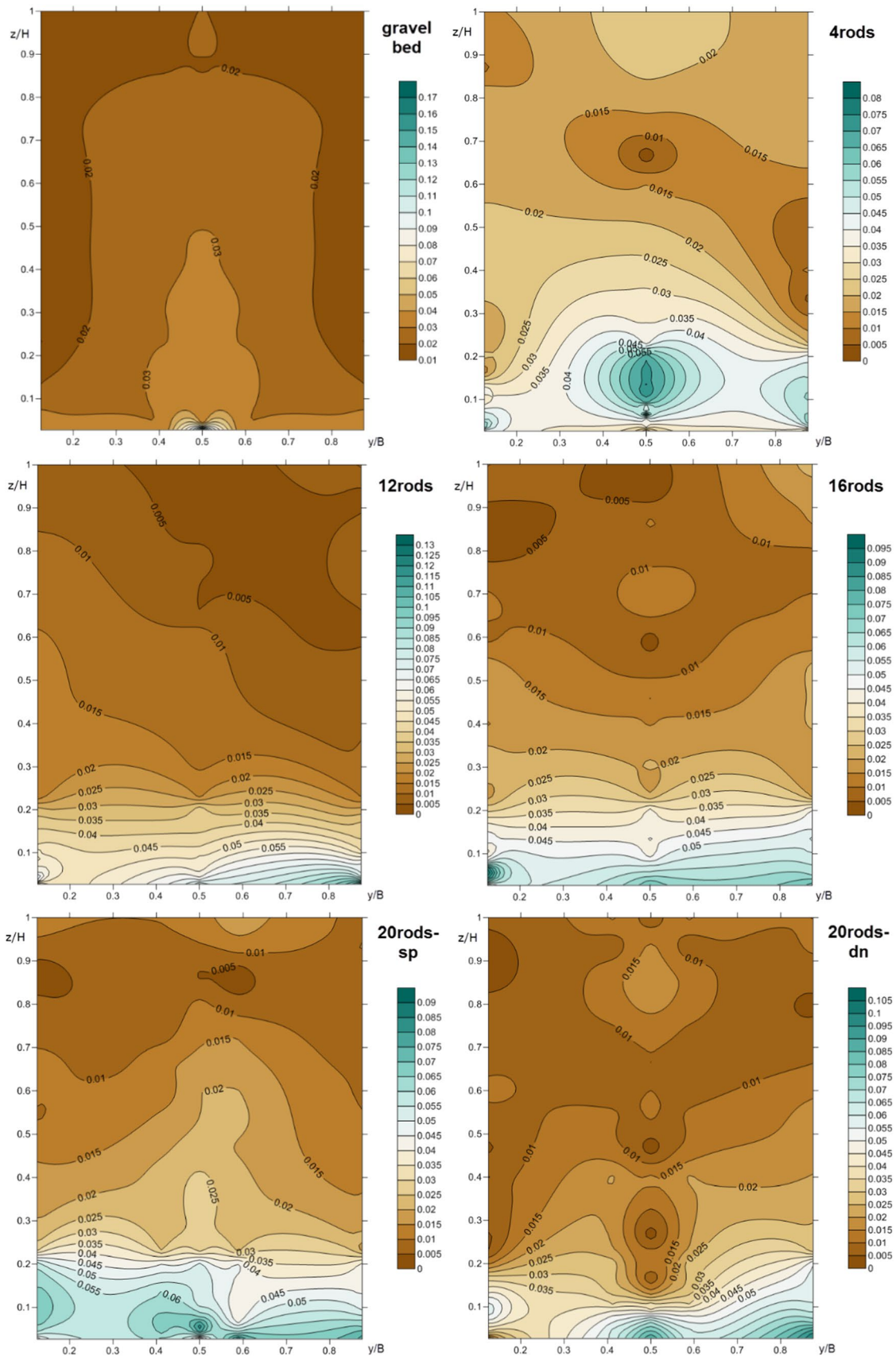


Fig. 4 Shear velocity calculated by Eq. 6 and Eq. 9 for different vegetation densities

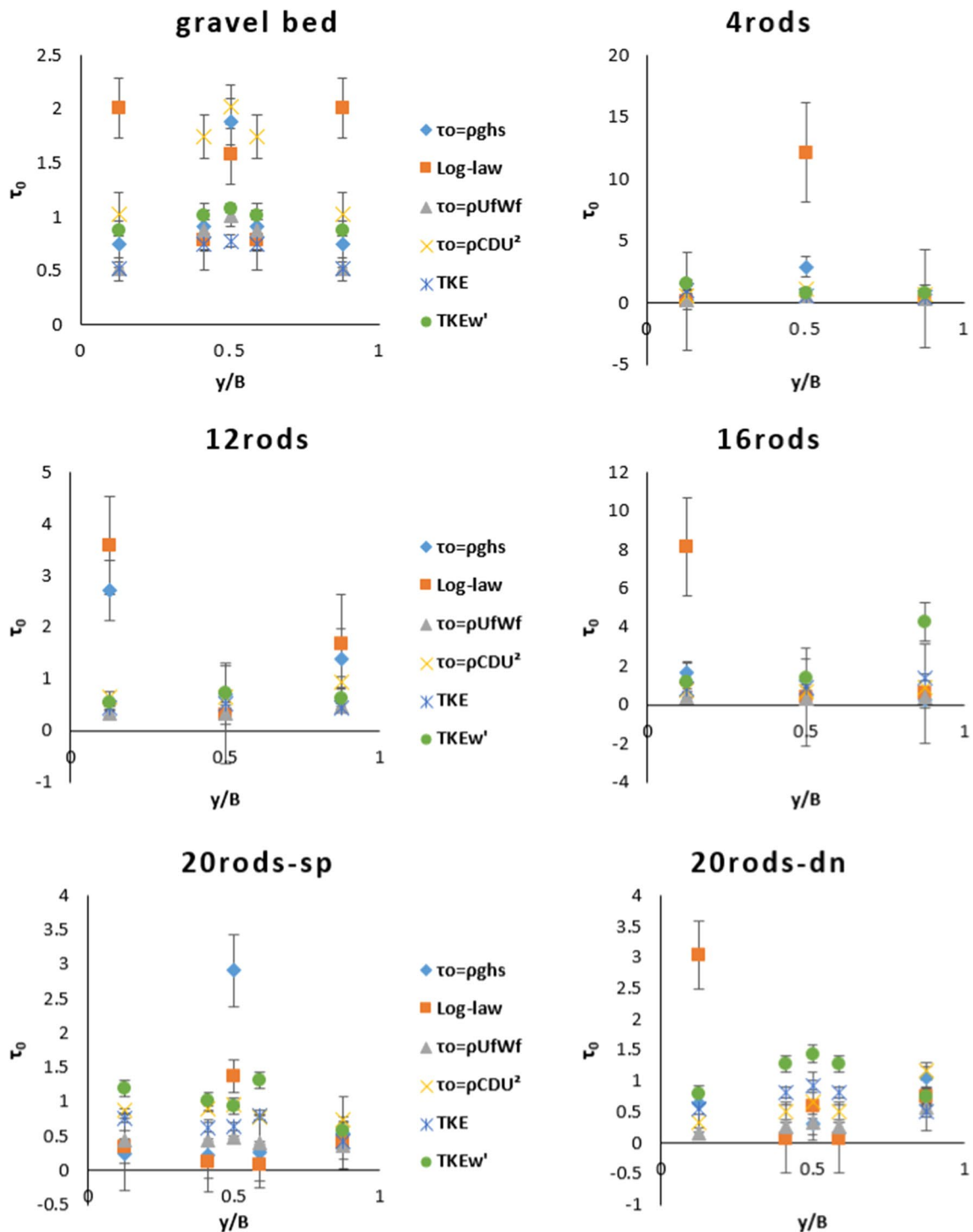


Fig. 5 A comparison of six methods of calculating bed shear stress

stress values varied slowly in the cross section of flume and were independent of the vegetation region and vegetation densities. This method seemed to be suitable for non-vegetation and vegetation cases.

From the log-law method, the highest bed shear stress value was obtained near the wall in the gravel bed and in vegetation cases it did not work regularly.

From the Reynolds stress method, the highest bed shear stress value was obtained in the ax axes for gravel bed and 4 rods density. For other vegetation cases, the distribution of

Table 1 A comparison of six methods of calculating bed shear stress

Run	Methods						
	$\tau_0 = \rho g h_s$	Log-law	$\tau_0 = \rho U_f W_f$	$\tau_0 = \rho C D U^2$	TKE	TKEw'	y/B
Gravel bed	0.749347	2.010626	0.514862	1.029724	0.525418	0.868784	0.125
	0.906529	0.788486	0.872433	1.744866	0.748657	1.017615	0.4125
	1.886855	1.58404	1.009818	2.019637	0.777323	1.081688	0.5
	0.906529	0.788486	0.872433	1.744866	0.748657	1.017615	0.5875
4 rods	0.749347	2.010626	0.514862	1.029724	0.525418	0.868784	0.875
	0.228225	0.118374	0.265543	0.531086	0.980572	1.595278	0.125
	2.880607	1.216168	0.537048	1.074097	0.600809	0.805761	0.5
12 rods	0.664246	0.361	0.312857	0.625714	0.488632	0.74253	0.875
	2.712097	3.585614	0.325043	0.650087	0.431746	0.546049	0.125
	0.714285	0.30276	0.321069	0.642139	0.519368	0.723793	0.5
16 rods	1.392126	1.667906	0.473708	0.947416	0.439705	0.614078	0.875
	1.686421	0.813604	0.382993	0.765985	0.842732	1.197412	0.125
	0.486989	0.39204	0.349033	0.698067	0.889703	1.38257	0.5
20 rods-sp	0.257836	0.583706	0.435663	0.871326	1.394222	4.293061	0.875
	0.237849	0.33709	0.433777	0.867553	0.759233	1.193985	0.125
	0.217721	0.114918	0.450415	0.90083	0.622295	1.007455	0.4125
20 rods-dn	2.9094	1.377894	0.479722	0.959443	0.638874	0.940078	0.5
	0.271792	0.086118	0.39293	0.78586	0.803895	1.314133	0.5875
	0.548683	0.403206	0.371166	0.742332	0.416122	0.585572	0.875
	0.636949	3.038214	0.16369	0.32738	0.542301	0.78531	0.125
	0.154657	0.064642	0.25935	0.5187	0.81722	1.276876	0.4125
	0.298928	0.587578	0.333473	0.666947	0.935656	1.437645	0.5
	0.154657	0.064642	0.25935	0.5187	0.81722	1.276876	0.5875
	1.05954	0.746382	0.578624	1.157248	0.501417	0.758318	0.875

bed shear stress values in the cross section of the flume was nearly the same. The bed shear stress values decreased when vegetation was added and densities increased. This method and first methods had the same results.

The results of the drag method are twice the results of the Reynolds shear stress method. The TKE and TKEW' methods were same because W' is more than U' and V' , the TKEW' method obtained larger values.

From Fig. 5 and Table 1, for non-vegetation gravel bed, the TKE and Reynolds stress methods obtained the lowest values. For vegetation cases, the Reynolds stress and log-law methods obtained the lowest values and TKEW' obtained the most values.

From the analysis presented above, the best method for non-vegetation and vegetation cases was the Reynolds stress method. Because it is obtained from turbulence fluctuations and flow is turbulent in all cases, this outcome can be regarded as plausible.

3.3 Velocity Distributions

Figure 6 shows streamwise velocity, U , within the cross section of the flume. On the gravel bed, streamwise velocity increased from bed toward flow surface as is in many

typical open channel flows. The velocity contours must be horizontal and parallel to each other, because of the influence of the walls and small width each value of U occurred in depth less in centerline of the flume than near the walls.

In Fig. 6, for the vegetated cases, dotted lines showed the location of the emergent rods used in the experiments. For the case of 4 rods, in $\frac{z}{H} < 0.1$, the velocity contours remained parallel to each other, but after that, changes in vertical and parallel lines and contours were dense because changes of values of velocity in the cross section were high. In the other words, in each $\frac{y}{B}$, over $\frac{z}{H} > 0.1$, the gradient of velocity is slowly changed, because of the existence of emergent vegetation that make the velocity fluctuation to reduce the momentum changed. There was this condition from the right wall to the centerline of the flume ($\frac{y}{B} = 0.5$).

For 12 rods and 16 rods, in $\frac{z}{H} < 0.1$, the velocity contours were horizontal and parallel and after that changes to vertical and parallel contours and changes of values of velocity in cross section were low.

For 20 rods all velocity contours were vertical over the flow depth but in 20 rods-dense contours were vertical and parallel.

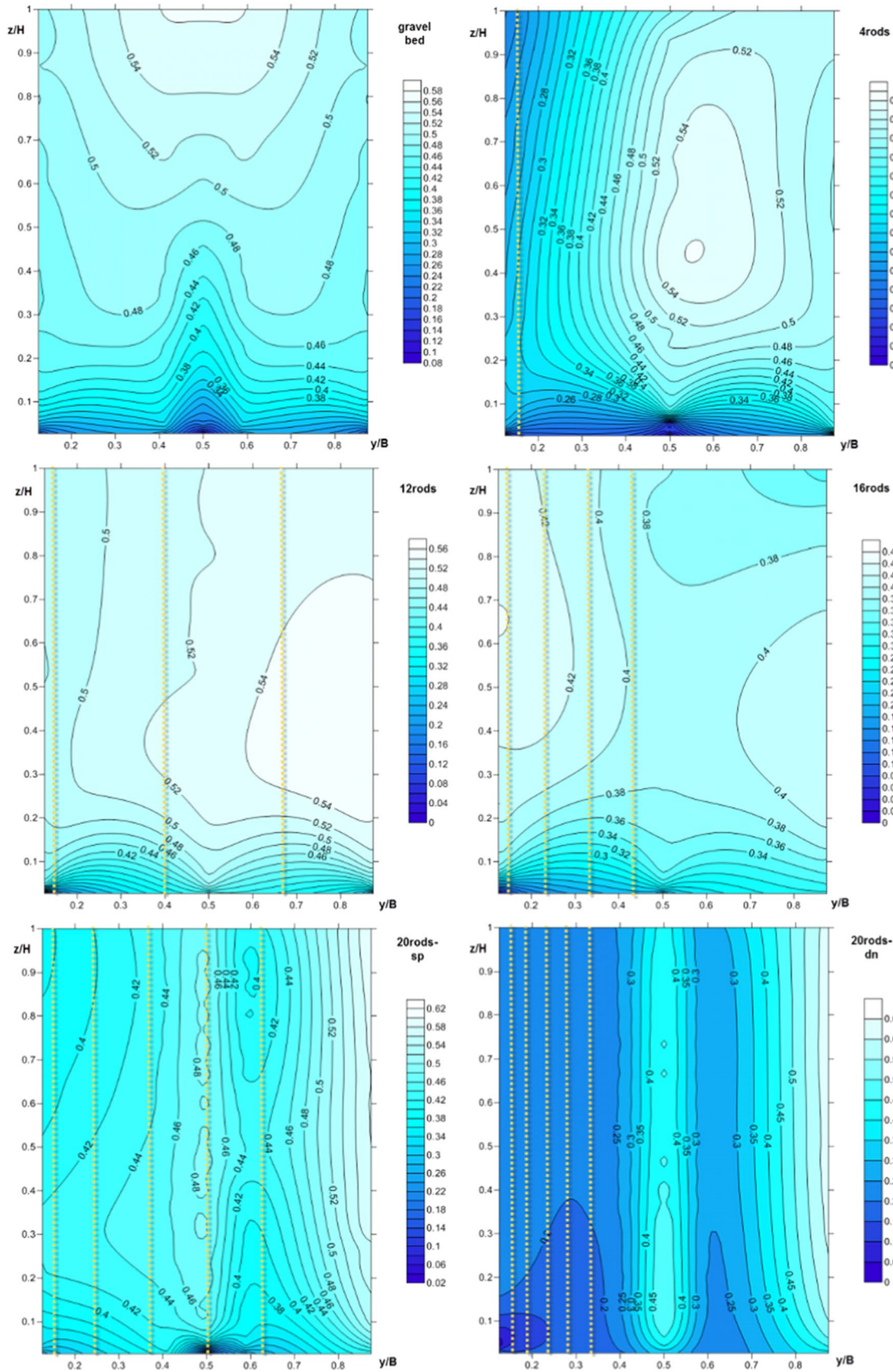


Fig. 6 Streamwise velocity in cross section of flume, U

Emergent circular rods channelized flow and with increasing densities, they made flow layers vertical and parallel over flow depth.

From Fig. 7, the transverse velocity, V , on the gravel bed, increased from negative values on the walls to maximum positive values in the centerline of flume toward flow surface. The rotation direction of the secondary flow was clockwise, because the transverse velocity varied from the negative to positive values along the y -direction (Liu et al. 2013). On gravel bed, the secondary flow rotated clockwise from the right wall and counterclockwise from the left wall in the y -direction horizontally. By adding emergent vegetation near the right wall, in the 4 rods case, the transverse velocity varied from negative values in the right region to positive values toward the left wall, so secondary flow rotation was clockwise horizontally in the y -direction. In the vegetation region, the transverse velocity contours were distributed vertically. In the 12 rods case, the cylinders were placed from the right wall to the centerline of flume. In this case, negative values occurred just on the bottom of flume slowly and the secondary flow rotated clockwise in the z -direction vertically. By increasing the density, for 16 rods and 20 rods, the secondary flow rotated clockwise in the z -direction vertically.

From Fig. 8, on the gravel bed, negative values of vertical velocity, W , occurred near the walls and zero and positive values occurred in centerline of flume toward the flow surface. In vegetation cases, when cylinders were placed more than half of the flume, 12 rods case, the vertical velocity values were negative mainly and just near the water surface occurred zero and positive values. The velocity contours in this case were parallel horizontally. In the other vegetation cases, the negative values occurred in the vegetation region and positive values and zero values occurred in the centerline toward the flow surface. So the walls of flume and emergent vegetation causes negative vertical velocity.

3.4 Turbulence Distribution

From Fig. 9, on gravel bed, turbulence, U' , decreased in the z -direction and the maximum turbulence occurred at the bottom of flume. When vegetation was added, the turbulence values increased in all vegetation cases and most values occurred in the vegetation region in the cross section.

It is conceivable that gravel and vegetation generated turbulence and changed from the uniform flow to non-uniform flow.

4 Conclusions

The following conclusions are drawn from this study:

1. The influence of emergent vegetation on flow pattern is like the wall of flume. Emergent vegetation divides flow between cylinders and changes flow layers from horizontal layers to vertical layers.
2. The shear stress is distributed in the z -direction in emergent vegetation like the distribution of shear stress in non-vegetation gravel bed near the walls of flume. The concave shear stress distribution in non-vegetation gravel bed far from the walls is unlike the vegetation cases.
3. It is proposed to calculate $(\frac{d\bar{U}}{dz} = \frac{U_i - U_{i-1}}{z_i - z_{i-1}})$ over the flow depth to obtain the viscous stress.
4. The shear velocity is obtained from the momentum equation and from the total stress distribution. In vegetation cases, there is a direct relationship between shear velocity and vegetation density (m) and frontal projected area of the stem (AV) that appears as the coefficient of Reynolds shear stress.
5. Near bottom of flume, shear stress changes highly so layers are denser and appears as an onion shape that we call "shear onion." In vegetation cases, the shear onion happen in $\frac{z}{H} < 0.3$ and after that changes are reduced. When vegetation is placed near the right wall of flume, the shear onion appears independent of region of vegetation. By increasing the density of vegetation, the shear onion is distributed from the centerline to the entire cross section of flume and high densities generate several onions.
6. This study investigates six methods to obtain the bed shear stress and the best method for non-vegetation and vegetation cases is found to be the Reynolds stress method. Because it is obtained from turbulence fluctuations and flow is turbulent in all cases.
7. For low density of cylinders, in $\frac{z}{H} < 0.1$, the velocity contours remain horizontal and parallel but after that changes to vertical and parallel lines and contours are dense, because changes in the values of velocity in the cross section are high. For high density of cylinders, all velocity contours are vertical over the flow depth but in 20 rods-dense contours are vertical and parallel.
8. The transverse velocity, V , in gravel bed, increases from negative values in the walls to the maximum positive values in the centerline toward the flow surface, so the secondary flow rotates clockwise and counterclockwise in the z -direction. For low density of cylinders, the secondary flow rotates in the y -direction horizontally and in high density of cylinders, it rotates in the z -direction vertically.

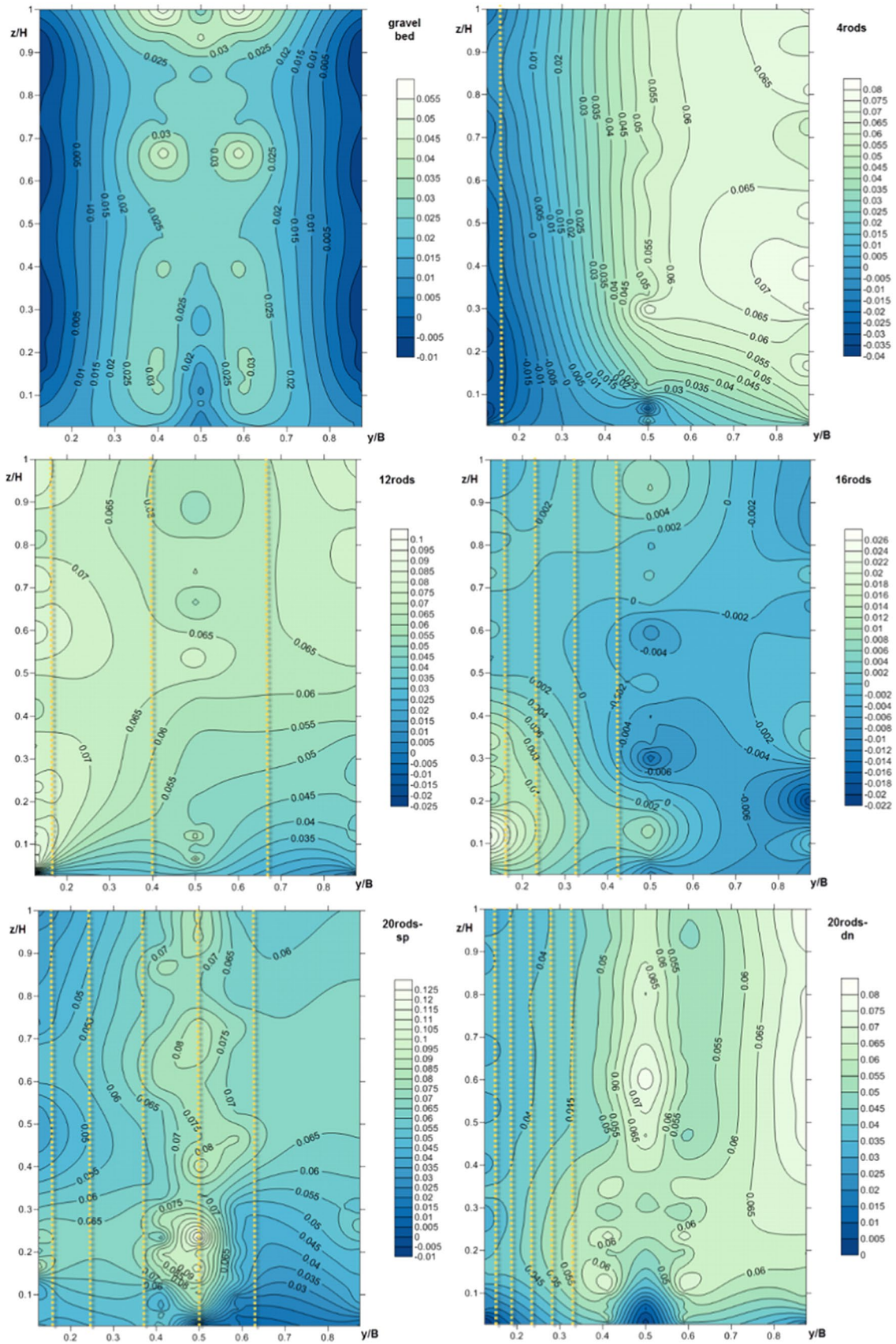


Fig. 7 Velocity in transverse directions of flume, V

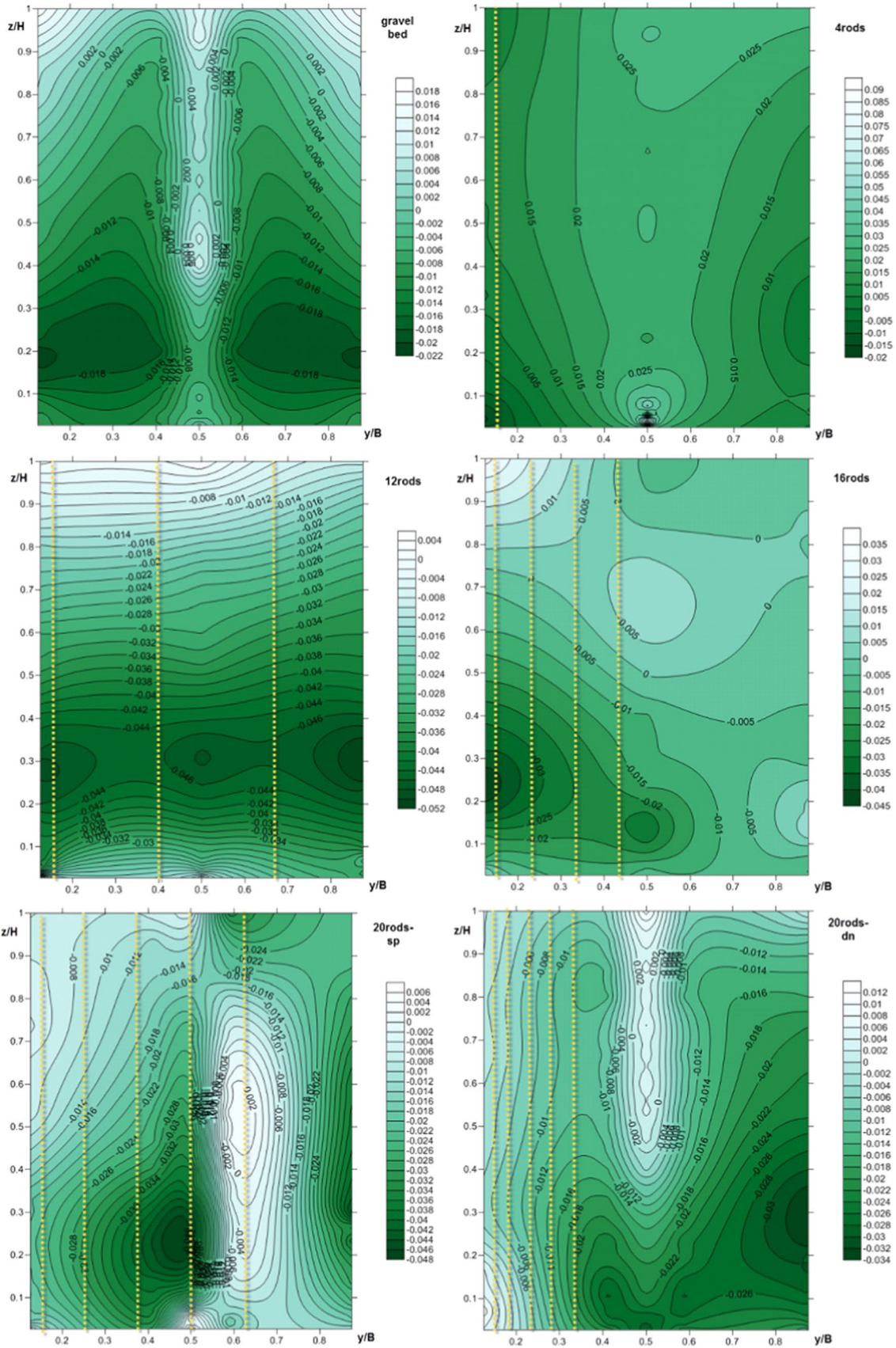


Fig. 8 Velocity in vertical directions of flume, W

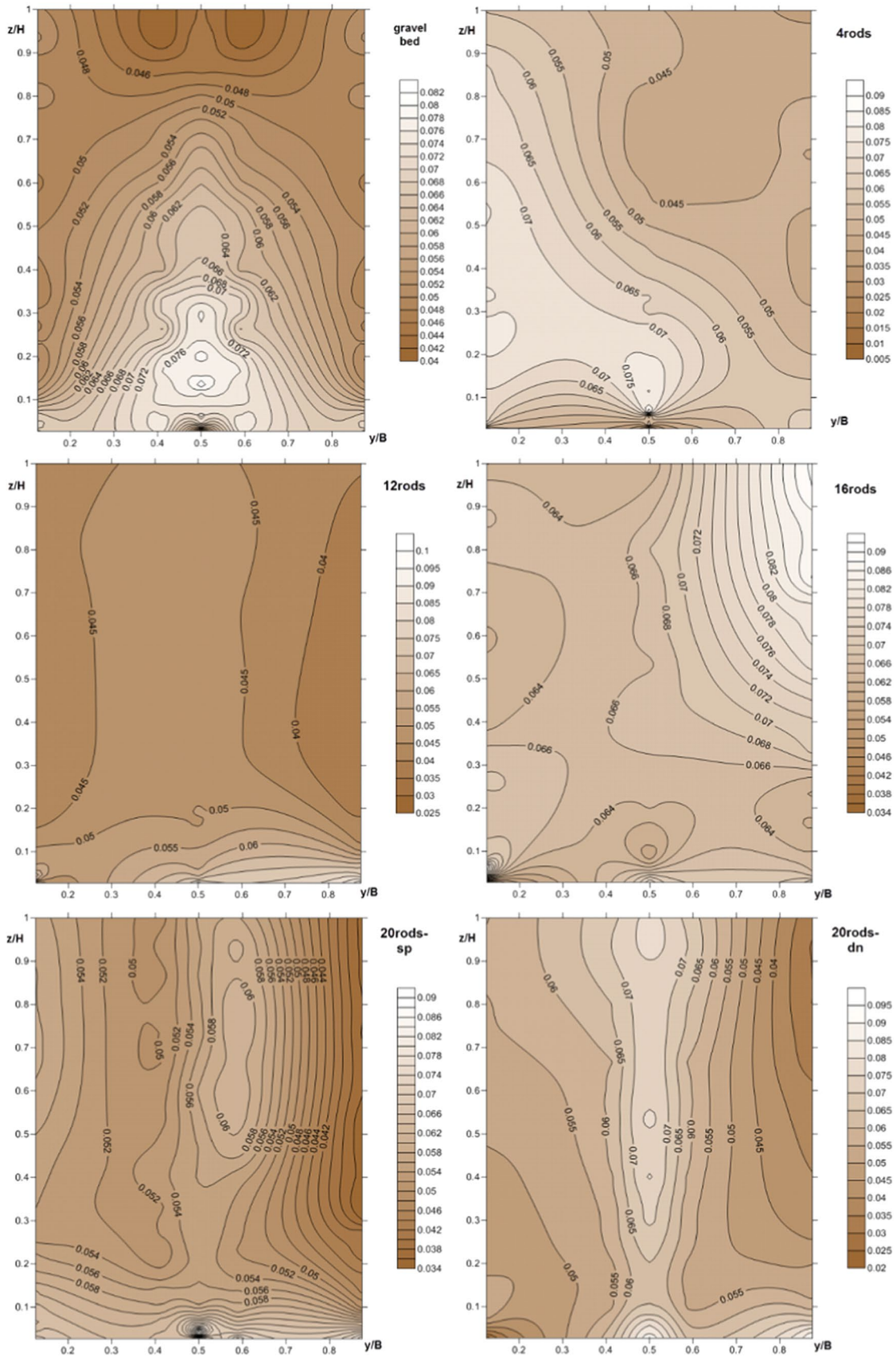


Fig. 9 Turbulence (U') distributions in cross section of flume

9. Probably due to adverse pressure gradient near walls of flume and emergent vegetation cause negative vertical velocity, W , and zero and positive values occur on the flow surface for gravel bed and for vegetation flow occur they in the non-vegetation region.
10. The similarity of RS and turbulence intensities distributions with the measured data for different densities is a great achievement showing if the high accuracy is not needed, the results of bare bed can be used for the conditions where reedy vegetation with different densities are prevalent. Of course, the Reynolds stress distribution can be used to estimate the bed shear stress and shear velocity and then evaluate the friction factor and the Shields parameter in sediment transport studies.

Acknowledgements We thank Dr. Oral Yagci reviewer for their useful comments.

References

- Afzalimehr H, Dey S (2009) Influence of bank vegetation and gravel bed on velocity and reynolds stress distributions. *Int J Sedi Res* 24(2):236–246
- Afzalimehr H, Setayesh P (2018) Investigation of logarithmic law and Coles' law for different emergent vegetation patches. *Iranian Hydra J* 13(1):47–62
- Afzalimehr H, Sui J, Moghbel R (2010a) Hydraulic parameters in channels with wall vegetation and gravel bed—field observations and experimental studies. *Int J Sed Res* 25(1):81–89
- Afzalimehr H, Fazel E, Singh VJ (2010b) Effect of vegetation on banks on distributions of velocity and reynolds stress under accelerating flow. *J Hydrol Eng Am Soc Civil Eng (ASCE)* 15(9):708–713
- Afzalimehr H, Fazel E, Ghalichand J (2012) Effects of accelerating and decelerating flows in a channel with vegetated banks and gravel bed. *Int J Sed Res* 27(2):188–200
- Afzalimehr H, Moradian M, Sui J, Gallichand J (2016) Effect of adverse pressure gradient and vegetated banks on flow structure. *J Riv Res and App*. <https://doi.org/10.1002/rra.2908>
- Afzalimehr H, Barahimi M, Sui j, (2019a) Non-uniform flow over cobble bed with submerged vegetation strip. *Proc Inst Civil Eng Water Manag* 172(2):86–101
- Afzalimehr H, Riazi P, Jahadi M, Singh VP (2019b) Effect of vegetation patches on flow structures and friction factor. *ISH J Hydra Eng*. <https://doi.org/10.1080/09715010.2019.1660920>
- Biron PM, Robson C, Lapointe MF, Gaskin SJ (2004) Comparing different methods of bed shear stress estimates in simple and complex flow fields. *Earth Surf Proc and Landforms* 29(11):1403–1415. <https://doi.org/10.1002/esp.1111>
- Brahimi M, Afzalimehr H (2019) Effect of submerged vegetation density on flow under favorable pressure gradient. *SN App Sci* 1(1):57
- Dey S (2014) *Fluvial Hydrodynamics: Hydrodynamic and Sediment Transport Phenomena*. Springer, Berlin
- Fazlollahi A, Afzalimehr H, Sui J (2015) Effect of slope angle of an artificial pool on distributions of turbulence. *J Int Sed Res* 30:93–99
- Fazlollahi A, Afzalimehr H, Sui J (2015) Impacts of pool and vegetated banks on turbulent flow characteristics. *Canadian J Civil Eng*. <https://doi.org/10.1139/cjce-2015-0172>
- Follett EM, Nepf HM (2012) Sediment patterns near a model patch of reedy emergent vegetation. *Geomorphology* 179:141–151
- Goring D, Nikora V (2002) Despiking acoustic doppler velocimeter data. *J Hydra Eng* 128(1):117–126
- Graf WH, Altinakar MS (1998) *Fluvial hydraulics-flow and transport processes in channels of simple geometry*. Wiley, New York
- Hamidifar H, Keshavarzi A, Rowiński PM, (2020) Influence of rigid emerged vegetation in a channel bend on bed topography and flow velocity field: laboratory experiments. *J Water* 12(1):118
- Huai WX, Zeng YH, Xu ZG, Yang ZH (2009) Three-layer model for vertical velocity distribution in open channel flow with submerged rigid vegetation. *Adv in Water Res* 32:487–492
- Huai W, Wang W, Hu Y, Zeng Y, Yang Z (2014) Analytical model of the mean velocity distribution in an open channel with double-layered rigid vegetation. *Adv in Water Res* 69:106–113
- Jahadi M, Afzalimehr H, Ashrafizade M, Kumar B (2020) A numerical study on hydraulic resistance in flow with vegetation patch. *ISH J Hydra Eng* 1–8
- Kitsikoudis V, Yagci O, Kirca VSO, Kellecioglu D (2016) Experimental investigation of channel flow through idealized isolated tree-like vegetation. *Environ Fluid Mech* 16:1283–1308. <https://doi.org/10.1007/s10652-016-9487-7>
- Kitsikoudis V, Yagci O, Kirca VSO (2020) Experimental analysis of flow and turbulence in the wake of neighboring emergent vegetation patches with different densities. *Environ Fluid Mech*. 20(6):1417–1439
- Klopstra D, Barneveld HJ, Noortwijk JM, Velzen EH (1997) Analytical model for hydraulic roughness of submerged vegetation. *Proc 27th IAHR Cong in San Francisco, USA*, 775–780
- Liu C, Luo X, Liu X, Yang K (2013) Modeling depth-averaged velocity and bed shear stress in compound channels with emergent and submerged vegetation. *Adv Water Res* 60:148–159
- Nasiri E, Afzalimehr H, Sui J (2010) Effect of vegetation channel banks on velocity distributions, characteristics of shear stress and turbulence intensities. *Int J Sed Res* 25(2):110–118
- Nasiri E, Afzalimehr H, Singh VP (2011) Effect of bed forms and vegetated banks on velocity distributions and turbulent flow structure. *J Hydro Eng ASCE* 16(6):495–507
- Nasiri Dehsorkhi E, Afzalimehr H, Gallichand J, Rousseau A (2013) Turbulence measurements above fixed gravel dunes. *Int J Hydra Eng* 2(5):101–114
- Neary VS (2003) Numerical solution of fully developed flow with vegetative resistance. *J Eng Mech* 129(5):558–563
- Righetti M (2008) Flow analysis in a channel with flexible vegetation using double averaging method. *Acta Geophy* 56(3):801–23. <https://doi.org/10.2478/s11600-008-0032-z>
- Righetti M, Armanini A (2002) Flow resistance in open channel flows with sparsely distributed bushes. *J Hydro* 269(1–2):55–64. [https://doi.org/10.1016/S0022-1694\(02\)00194-4](https://doi.org/10.1016/S0022-1694(02)00194-4)
- Sellin RHJ, Vanbeesten DP (2004) Conveyance of a managed vegetated two stage river channel. *Proc Inst Civil Eng Water Manag* 157(1):21–33. <https://doi.org/10.1680/wama.2004.157.1.21>
- Shahmohammadi R, Afzalimehr H, Sui J (2018) Interaction of turbulence and vegetation patch on the incipient motion of sediment. *Canadian J Civil Eng* 45(9):803–816
- Shimizu Y, Tsujimoto T (1994) Numerical analysis of turbulent open-channel flow over a vegetation layer using a k - ϵ turbulence model. *J Hydrosc and Hydra Eng* 11(2):57–67
- Tang H, Tian Z, Yan J, Yuan S (2014) Determining drag coefficients and their application in modelling of turbulent flow with submerged vegetation. *Adv in Water Res* 69:134–145
- Thompson AM, Wilson BN, Hansen BJ (2004) Shear stress partitioning for idealized vegetated surfaces. *Trans ASAE*. 47(3):701–99

- Wilson C (2007) Flow resistance models for flexible submerged vegetation. *J Hydrol* 342(3–4):213–222
- Wilson C, Yagci O, Rauch HP, Stoesser T (2006) Application of the drag force approach to model the flow interaction of natural vegetation. *Int J River Basin Manag* 4(2):137–146. <https://doi.org/10.1080/15715124.2006.9635283>
- Wilson C, Yagci O, Rauch HP et al (2006) 3D numerical modeling of a willow vegetated river/floodplain system. *J Hydrol* 327(1–2):13–21
- Wolman MG (1954) A method of sampling coarse riverbed material. *J Trans-Am Geophysc Union* 35:951–956
- Yagci O, Kabdasli M (2008) The impact of single natural vegetation elements on flow characteristics. *Hydrol Proc* 22:4310–4321
- Yagci O, Celik MF, Kitsikoudis V, Kirca VO, Hodoglu C, Valyrakis M, Duran Z, Kaya S (2016) Scour patterns around isolated vegetation elements. *J Adv Water Resour* 97:251–265. <https://doi.org/10.1016/j.advwatres.2016.10.002>
- Yagci O, Yildirim I, Celik MF, Kitsikoudis V, Duran Z, Kirca VSO (2017) Clear water scour around a finite array of cylinders. *Appl Ocean Res*. 68:114–129. <https://doi.org/10.1016/j.apor.2017.08.014>
- Yang JQ, Kerger F, Nepf HM (2015) Estimation of the bed shear stress in vegetated and bare channels with smooth beds. *Water Resour Res* 51(5):3647–3663. <https://doi.org/10.1002/2014WR016042>